Applied Clay Science 91–92 (2014) 1–5

Contents lists available at ScienceDirect

Applied Clay Science

journal homepage: www.elsevier.com/locate/clay

Research paper

Using Agrawal integral equation, dynamic mechanical analysis (DMA), and differential scanning calorimeter (DSC) methods to study the glass transition kinetics of nanocomposites of polybenzoxazine and exfoliated montmorillonite from a polyhedral oligomeric silsesquioxane surfactant and click chemistry

Hui-Wang Cui [a,b,*], Shiao-Wei Kuo [a]

[a] Department of Materials and Optoelectronic Science, National Sun Yat-Sen University, Kaohsiung 804, Taiwan
[b] Institute of Scientific and Industrial Research, Osaka University, Suita 565-0871, Osaka, Japan

ARTICLE INFO

Article history:
Received 27 March 2013
Received in revised form 15 January 2014
Accepted 24 January 2014
Available online xxxx

Keywords:
Nanocomposites
Polybenzoxazine
Glass transition
Kinetics

ABSTRACT

In this study, we used a singly azido-functionalized polyhedral oligomeric silsesquioxane (POSS) derivative and a montmorillonite intercalated by propargyldimethylstearylammonium bromide to prepare an exfoliated montmorillonite through click chemistry. This exfoliated montmorillonite was then introduced into a benzoxazine matrix prepared from paraformaldehyde, aniline, and phenol to form polybenzoxazine/exfoliated clay nanocomposites. Dynamic mechanical analysis, differential scanning calorimetry, and Agrawal integral equation revealed that the glass transition kinetics had a close relationship to the structure, assembly process, and anchoring effect of montmorillonite layers, the compatibility between polybenzoxazine and intercalator, and the methods of dynamic mechanical analysis and differential scanning calorimetry. The polybenzoxazine/exfoliated clay nanocomposites presented the same mechanism function at different weight ratios between polybenzoxazine and exfoliated clay, and the kinetic compensation effect equations revealed the nature of glass transition.

1. Introduction

Polybenzoxazines have been studied widely ever since they were first reported (Holly and Cope, 1944), with various related applications appearing gradually (Baqar et al., 2011; Ishida, 2011, Wang et al., 2006a, b, 2007, 2011; Yang and Gu, 2011). They exhibit many unique properties, such as near-zero volume changes upon polymerization with high mechanical integrity, low water adsorption in water at room temperature, surprisingly high glass transition temperatures (T_g), rapid development of physical and mechanical properties during polymerization processes (e.g., 80% of the T_g development occurs at a 50% degree of conversion for a bisphenol-A/aniline–based benzoxazine), very high char yields, and low surface energies (Ishida and Allen, 1996; Ishida and Low, 1997; Jin et al., 2010; Kanchanasopa et al., 2001; Kiskan et al., 2011; Kuo et al., 2009; Wang et al., 2006a,b). For further improving the physical properties of polybenzoxazines, one of the most important technologies is to manufacture the (nano)composites through blending with other polymers or nanofillers (Huang et al., 2007; Kuo and Liu, 2010; Su et al., 2003). These (nano)composites can impart polybenzoxazines with excellent processability and superb mechanical properties without forming any volatile species. Although many reports have described nanocomposites manufactured through the incorporation of clay into polybenzoxazines, in those cases the clay minerals are merely intercalated and dispersed in the polymeric matrix with a layered structure (Agag and Takeichi, 2008; Chozhan et al., 2009; Fu et al., 2008; Garea et al., 2009; Sudo et al., 2008).

In this study, we used polyhedral oligomeric silsesquioxane (POSS) nanocomposites to improve the exfoliation of clay incorporated in a polybenzoxazine. POSS derivatives, unlike most silicones or fillers, are cage-like molecules presenting organic substituents on their outer surfaces that let them be compatible or miscible with most polymers. These functional groups can be designed either as non-reactive for blending or reactive for polymerization (Chandramohan et al., 2012; Chou et al., 2005a,b; Song et al., 2012; Wang et al., 2012). Therefore, after intercalating propargyl dimethylstearylammonium bromide into the layers of montmorillonite (Mt) to form intercalated montmorillonite (In-Mt), we introduced a mono-functionalized azide-POSS derivative to undergo click reactions with the acetylenic intercalator units, resulting in the exfoliation of Mt into nanoparticles in the form of single layers (Cui and Kuo, 2012). We then incorporated this exfoliated montmorillonite (Ex-Mt) into the Pa-type benzoxazine (3-phenyl-3,4-dihydro-2H-benzoxazine) monomer-derived from paraformaldehyde, aniline,

* Corresponding author at: Institute of Scientific and Industrial Research, Osaka University, Suita 565-0871, Osaka, Japan. Tel.: +81 6 6879 8521; fax: +81 6 6879 8522.
E-mail address: cuihuiwang@hotmail.com (H.-W. Cui).

http://dx.doi.org/10.1016/j.clay.2014.01.016
0169-1317

and phenol-to form exfoliated polybenzoxazine nanocomposites (Cui and Kuo, 2013), the glass transition kinetics of which we investigated using Agrawal integral equation, dynamic mechanical analysis (DMA), and differential scanning calorimetry (DSC).

2. Experiments

2.1. Samples

The pristine montmorillonite (Mt) was purchased from Nanocor (USA). The Pa-type benzoxazine (3-phenyl-3,4-dihydro-2H-benzoxazine) monomer, In-Mt, and Ex-Mt were prepared according to previously reported procedures. The Pa-type benzoxazine monomer was prepared from paraformaldehyde, aniline, and phenol (Huang and Kuo, 2010; Ishida, 2011); In-Mt from pristine Mt, *N*,*N*-dimethylstearylamine, and propargyl bromide (Cui and Kuo, 2012); and Ex-Mt from In-Mt and mono-functionalized azide-POSS derivative through click chemistry (Cui and Kuo, 2012; Hu et al., 2012; Lin and Kuo, 2011, 2012).

The polybenzoxazine/clay nanocomposites were prepared in the following processes (Cui and Kuo, 2013): Pa-type benzoxazine monomer was mixed with Mt, In-Mt, or Ex-Mt with vigorous stirring until the sample had become homogeneous; the sample was then placed in a natural oven and cured at 140 °C for 3 h, 160 °C for 3 h, and then 200 °C for 4 h under a heating rate of 2 °C · min^{-1}. As Table 1 shows, BM was formed from Pa polybenzoxazine and pristine Mt; BIM from Pa polybenzoxazine and In-Mt; and BEM from Pa polybenzoxazine and Ex-Mt. The weight ratio of Mt or In-Mt to Pa polybenzoxazine was fixed at 5%; those of Ex-Mt to Pa polybenzoxazine were 1%, 3%, 5%, 7%, and 10%, named BEM-A, BEM-B, BEM-C, BEM-D, and BEM-E, respectively.

2.2. Characterization

The glass transitions of the samples were investigated using a PerkinElmer DMA800 dynamic mechanical analyzer operated in air. The sample (10 mm × 8 mm × 2 mm) was fixed on the bracket and subjected to the single-frequency/strain mode as the temperature was increased from 25 to 200 °C at a rate of 2 °C · min^{-1}. Then they were also investigated using a TA Q-20 differential scanning calorimeter operated under an atmosphere of pure N_2. The sample (ca. 7 mg) was placed in a sealed aluminum sample pan. The glass transition scans were conducted from 25 to 250 °C at a rate of 20 °C · min^{-1}.

3. Results and discussion

In the glass transition kinetics, the mechanism function of $G(a)$ is:

$$G(a) = \frac{A}{\beta}\int_{T_0}^{T} e^{-\frac{E}{RT}} dT.$$

The Agrawal approximate equation is (Agrawal, 1987):

$$\int_{T_0}^{T} e^{-\frac{E}{RT}} dT = \frac{RT^2}{E}\left[\frac{1-\left(\frac{RT}{E}\right)}{1-5\left(\frac{RT}{E}\right)^2}\right] e^{-\frac{E}{RT}}.$$

Table 1
Compositions of polybenzoxazine/clay nanocomposites.

	BM	BIM	BEM-A	BEM-B	BEM-C	BEM-D	BEM-E
Pa	5 g	5 g	5 g	5 g	5 g	5 g	5 g
Mt	0.25 g	–	–	–	–	–	–
In-Mt	–	0.25 g	–	–	–	–	–
Ex-Mt	–	–	0.05 g	0.15 g	0.25 g	0.35 g	0.50 g

Combining the above two equations, the Agrawal integral equation is:

$$\ln\left[\frac{G(a)}{T^2}\right] = \ln\left\{\frac{AR}{\beta E}\left[\frac{1-\left(\frac{RT}{E}\right)}{1-5\left(\frac{RT}{E}\right)^2}\right]\right\} - \frac{E}{RT}.$$

For the general reaction temperatures and most E, the relationship among E, R, and T are:

$$\frac{E}{RT} >> 1, \quad 1-\left(\frac{RT}{E}\right) \approx 1, \text{ and } \quad 1-5\left(\frac{RT}{E}\right)^2 \approx 1.$$

The Agrawal integral equation is simplified as:

$$\ln\left[\frac{G(a)}{T^2}\right] = \ln\left(\frac{AR}{\beta E}\right) - \frac{E}{RT}.$$

The $\ln\left[\frac{G(a)}{T^2}\right]$ and $\frac{1}{T}$ can be fit linearly with a suitable $G(a)$. The E can be calculated from the linear slope and the A from the linear intercept. In the above equations, T (K) is the temperature, R is the universal gas constant at 8.314 J · $(mol \cdot K)^{-1}$, β (K · min^{-1}) is the heating rate, E (kJ · mol^{-1}) is the activation energy, A (min^{-1}) is the frequency factor, and a is the relative elastic modulus calculated by:

$$a = \frac{E'_{onset} - E'}{E'_{onset} - E'_{offset}}$$

where E'_{onset} (Pa) is the elastic modulus at onset temperature, E'_{offset} (Pa) is the elastic modulus at offset temperature, and E' is the elastic modulus at a temperature (Fig. 1(a) and (c)).

Or a is the relative heat flow calculated by:

$$a = \frac{H_{onset} - H}{H_{onset} - H_{offset}}$$

where H_{onset} (w · g^{-1}) is the heat flow at onset temperature, H_{offset} (w · g^{-1}) is the heat flow at offset temperature, and H (w · g^{-1}) is the heat flow at a temperature (Fig. 2).

According to the simplified Agrawal integral equation, T and a in the glass transition of Pa polybenzoxazine, BM, BIM, and BEM (Figs. 1 and 2) were fit linearly using a trial-and-error method (Hu and Shi, 2001). Tables S1 to S8 present the fit results from the DMA method and Tables S9 to S16 from the DSC method. On the basis of the linearly dependent coefficient (r), the glass transition kinetics of Pa polybenzoxazine, BM, BIM, and BEM was obtained and listed in Tables 2 and 3.

$G(a)$ is the kinetics mechanism function illustrating the glass transition process. It determines the linear fit equation, r, E, and A. If the $G(a)$ is different, others are definitely different. As shown in Tables 2 and 3, the $G(a)$ obtained through DMA and DSC methods was the same for Pa polybenzoxazine, BM, BIM, and BEM. All was $(1 - a)^{-1} - 1$, indicating that the glass transition only happened on the polymeric matrix of Pa polybenzoxazine. The pristine Mt, In-Mt, Ex-Mt, and testing methods did not influence the $G(a)$.

The E and A did not display the same cases as the $G(a)$. E is the required minimum energy for the molecules from a reactant state to an activated state in chemical reactions. In the glass transition, it is the different energy between the onset point and the offset point. A is a constant determined by the reaction nature and there is nothing to do with the reaction temperature and concentration in the system. E and A always present the same variation trends in the kinetics. If the E increases, the A will increase, and vice versa. As Tables 2 and 3 show, the Pa polybenzoxazine presented lower values of E and A than BM, BIM, and BEM because of their different transferring modes for heat and mass. The heat passed directly through the polymeric chains and

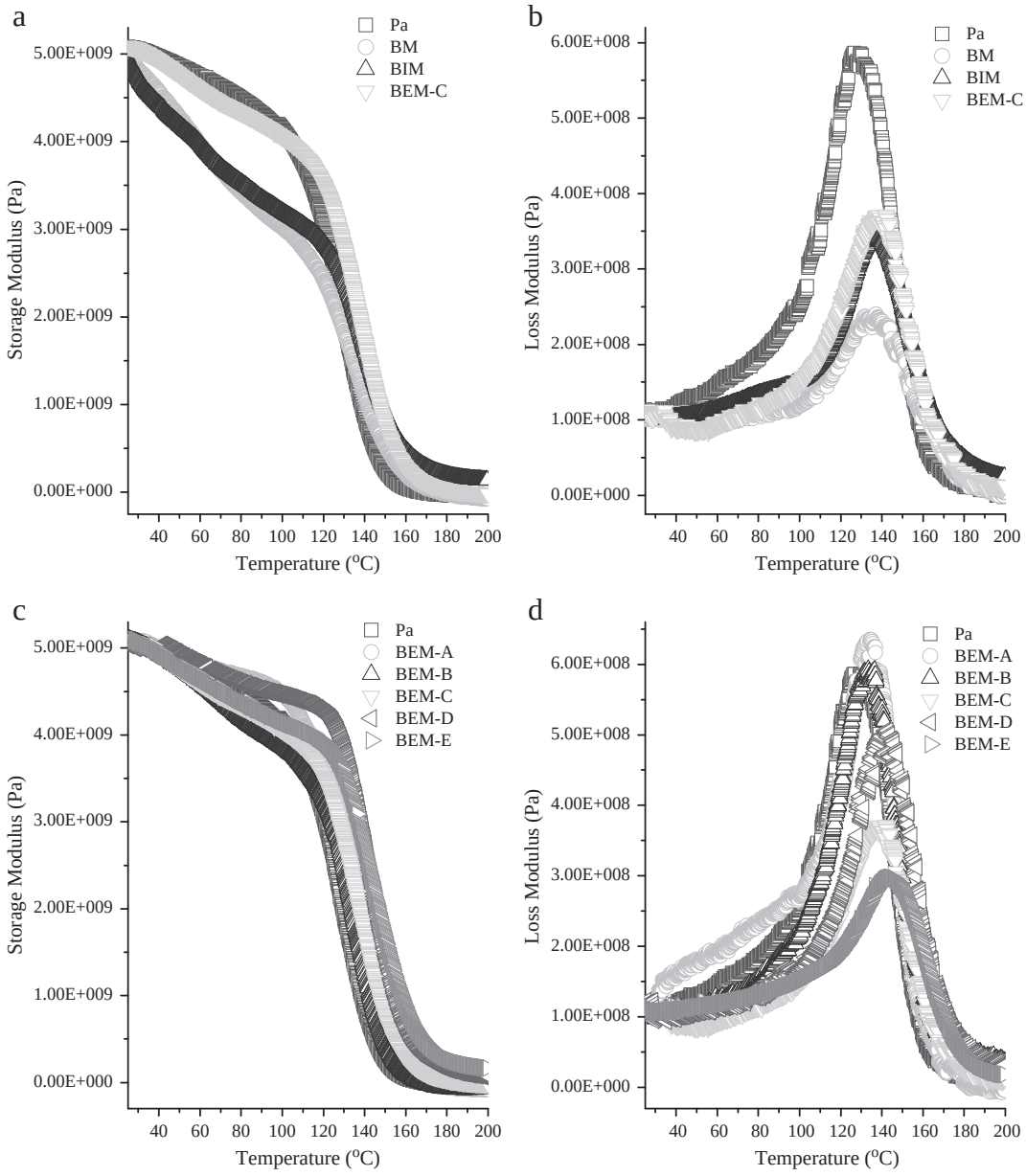

Fig. 1. DMA data revealing the (a, c) storage and (b, d) loss moduli of Pa, BM, BIM, BEM-C, and Pa polybenzoxazine samples containing various contents of Ex-Mt (BEM).

segments in Pa polybenzoxazine that allowed them to move freely and resulted in sharp changes of modulus and heat flow to lead rapid glass transitions. The transferring paths for the heat in BM, BIM, and BEM were delayed, blocked, or distorted as a result of the incorporation of pristine Mt, In-Mt, and Ex-Mt, respectively, into the polybenzoxazine matrix. These variations on the heat transferring paths caused the slow decrease or delayed the sharp changes for moduli and heat flows of BM, BIM, and BEM. Thus, more energy was required to conduct and complete the glass transition, which could provide higher *E* and *A*. The BM, BIM, and BEM also presented higher T_g values than Pa polybenzoxazine (Figs. 1 and 2, Tables 2 and 3) as they samely did for *E* and *A*.

It also can be seen that the Pa polybenzoxazine, BM, BIM, and BEM presented lower values of *E* and *A* obtained through the DMA method than those obtained through the DSC method (Tables 2 and 3), as would be expected because the molecules had to move significantly to change the modulus by several orders of magnitude to undergo the glass transition; that means that the glass transition changed gently and slowly using the DMA method, while it sharply and rapidly use the DSC method. This also can be indicated by that the values of T_g obtained through the DMA method were delayed (i.e., higher temperatures) relative to those obtained through the DSC method (Figs. 1 and 2, Tables 2 and 3).

The effect of pristine Mt, In-Mt, and Ex-Mt, and their weight ratios on the *E* and *A* is much more complicated and difficult to clarify, and may be related closely to their structures, especially with regard to their dispersion degree in the polymeric matrix. The pristine Mt had a layered structure, In-Mt was an intercalated nanocomposite, and Ex-Mt was an exfoliated nanocomposite; therefore, each was dispersed in the polybenzoxazine matrix in a different state (Cui and Kuo, 2012, 2013). The primary building blocks of the nanodomains of pristine Mt consisted of an assembly of many layers, arranged compactly and densely in a certain direction. In-Mt had a similar, or possibly even the same, layered morphology as that of pristine Mt, but the arrangement was not as compact or dense as that of pristine Mt. Ex-Mt did not have a layered structure; the Mt had been exfoliated into nanoparticles, or called single layers, as a result of the click reactions of the cage-like POSS nanoparticles. These single layers were dispersed randomly and freely in the polymeric matrix, and formed different dispersion states, such as the

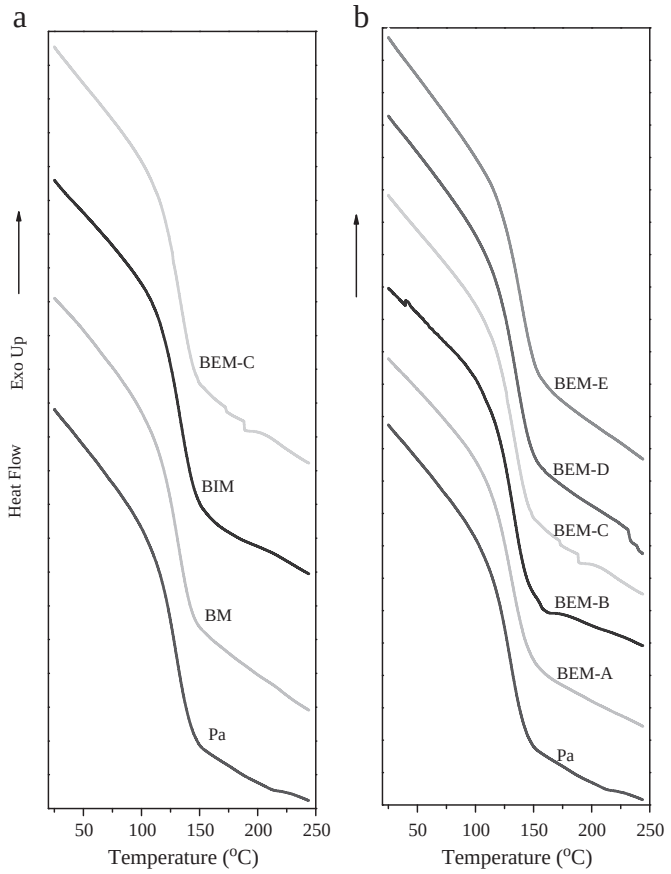

Fig. 2. DSC curves of (a) Pa, BM, BIM, and BEM-C and (b) Pa polybenzoxazine samples containing various contents of Ex-Mt (BEM).

so-called "random dispersion" and "island dispersion". Moreover, the random and island dispersions always appeared together in the form of the mixed dispersion (Cui and Kuo, 2013). The Ex-Mt-based nanocomposites often contained more than one dispersion of the exfoliated single layers. During the intercalation process leading to the formation of In-Mt, the exfoliation and click reactions leading to Ex-Mt, and the strong stirring in the preparation of BEM, the Mt was exfoliated into nanoparticles in the form of thin solid layers, elementary particles, or aggregates of the two. The Ex-Mt nanoparticles and polybenzoxazine chains also underwent an assembly process during the strong stirring for preparing BEM. The different charges of the components led to the formation of ionic bonds between them. This assembly process not only had a further exfoliation effect on the Ex-Mt nanoparticles but also anchored these exfoliated single layers with polybenzoxazine chains through physical crosslinking. In addition, the Ex-Mt nanoparticles also interacted with the polybenzoxazine chains indirectly as a result of the latter's compatibility with propargyldimethylstearylammonium bromide. In a word, the structure, assembly process, and anchoring effect of Mt layers, the compatibility of polybenzoxazine and intercalator, and the methods of DMA and DSC all combined together and let the BM, BIM, and BEM systems possess different values of E and A (Tables 2 and 3).

Table 2
Glass transition kinetics of Pa, BM, BIM, and BEM obtained through DMA method.

	$G(a)$	E (kJ · mol^{-1})	A (min^{-1})	T_g (°C)	k_g (min^{-1})
Pa	$(1-a)^{-1}-1$	193.70	6.17×10^{24}	130	0.4925
BM	$(1-a)^{-1}-1$	214.94	8.92×10^{26}	135	0.2701
BIM	$(1-a)^{-1}-1$	239.48	5.56×10^{29}	137	0.1758
BEM-A	$(1-a)^{-1}-1$	279.87	1.95×10^{35}	134	0.2417
BEM-B	$(1-a)^{-1}-1$	263.15	1.54×10^{33}	136	0.3899
BEM-C	$(1-a)^{-1}-1$	214.96	8.29×10^{26}	140	0.5497
BEM-D	$(1-a)^{-1}-1$	252.99	1.50×10^{31}	143	0.2630
BEM-E	$(1-a)^{-1}-1$	223.09	2.31×10^{27}	145	0.3123

Table 3
Glass transition kinetics of Pa, BM, BIM, and BEM obtained through DSC method.

	$G(a)$	E (kJ · mol^{-1})	A (min^{-1})	T_g (°C)	k_g (min^{-1})
Pa	$(1-a)^{-1}-1$	241.99	1.04×10^{32}	129	3.8388
BM	$(1-a)^{-1}-1$	299.66	2.81×10^{39}	131	5.2185
BIM	$(1-a)^{-1}-1$	260.27	1.63×10^{34}	133	5.4683
BEM-A	$(1-a)^{-1}-1$	282.34	1.60×10^{37}	132	6.3336
BEM-B	$(1-a)^{-1}-1$	289.29	1.19×10^{38}	132	5.9842
BEM-C	$(1-a)^{-1}-1$	309.62	3.94×10^{40}	134	7.4451
BEM-D	$(1-a)^{-1}-1$	289.44	7.17×10^{37}	136	7.9886
BEM-E	$(1-a)^{-1}-1$	294.89	1.58×10^{38}	140	8.2093

The aforementioned factors also influenced the reaction rate constant (k) calculated by Arrhenius equation:

$$k = Ae^{-\frac{E}{RT}}$$

k is related closely to the reaction temperature, reaction medium (or solvent), catalyst, etc., even to the shape and characteristics of reactors. Thus, the k at T_g (k_g) changed accordingly as the variations of E, A, T_g, and the methods of DMA and DSC (Tables 2 and 3).

The kinetic compensation effect indicates a linear relationship between ln$A$ and E that A compensates to the change of E partly (Hu and Shi, 2001):

$$\ln A = KE + Q$$

where K and Q are the kinetic compensation effect parameters calculated from the linear fit between E and A.

Table 4 shows the kinetic compensation effect equations of Pa polybenzoxazine, BM, BIM, and BEM. The K was the same at 0.0003 which coincided well with the kinetics mechanism function of $G(a)$. The same K also indicated that the glass transition mainly happened on the polymeric matrix of Pa polybenzoxazine. The Q presented negative values for Pa polybenzoxazine, BM, BIM, and BEM from the DMA method, and positive values from the DSC method. These differences were caused by the different characterization methods. In addition, the absolute values of Q at <2 were very small compared to 0.0003E, so the differences of the Q seemed to be neglected. Similarly, the Q was also influenced by the structure, assembly process, and anchoring effect of Mt layers, the compatibility of polybenzoxazine and intercalator, and the methods of DMA and DSC. It changed accordingly with E, A, and k_g. Because the K and Q are not affected by experimental factors, the kinetic compensation effect equations can explain the glass transition processes and reveal the glass transition natures of Pa polybenzoxazine, BM, BIM, and BEM, and also their theoretical expressions.

Table 4
Kinetic compensation effect equations of Pa, BM, BIM, and BEM.

	Kinetic compensation effect equation	
	Obtained through DMA	Obtained through DSC
Pa	$\ln A = 0.0003E - 0.8508$	$\ln A = 0.0003E + 0.7597$
BM	$\ln A = 0.0003E - 0.5410$	$\ln A = 0.0003E + 0.1448$
BIM	$\ln A = 0.0003E - 1.4905$	$\ln A = 0.0003E + 0.4407$
BEM-A	$\ln A = 0.0003E - 1.9785$	$\ln A = 0.0003E + 0.2093$
BEM-B	$\ln A = 0.0003E - 1.7252$	$\ln A = 0.0003E + 0.1777$
BEM-C	$\ln A = 0.0003E - 1.1856$	$\ln A = 0.0003E + 0.2409$
BEM-D	$\ln A = 0.0003E - 1.5649$	$\ln A = 0.0003E + 0.1779$
BEM-E	$\ln A = 0.0003E - 1.2224$	$\ln A = 0.0003E + 0.1627$

4. Conclusions

In this study, we investigated the glass transition kinetics of Pa polybenzoxazine, BM, BIM, and BEM using the Agrawal integral equation, DMA, and DSC. The glass transition kinetics had a close relationship to the structure, assembly process, and anchoring effect of Mt layers, the compatibility of polybenzoxazine and intercalator, and the methods of DMA and DSC. The Pa polybenzoxazine, BM, BIM, and BEM all had the same $G(a)$ of $(1-a)^{-1}-1$ and the same kinetic compensation effect parameter of K at 0.0003, indicating that the glass transition mainly happened on the polymeric matrix of Pa polybenzoxazine, and the kinetic compensation effect equations revealed their glass transition natures.

Appendix A. Supplementary data

Supplementary data to this article can be found online at http://dx.doi.org/10.1016/j.clay.2014.01.016.

References

Agag, T., Takeichi, T., 2008. Preparation and cure behavior of organoclay-modified allyl-functional benzoxazine resin and the properties of their nanocomposites. Polym. Compos. 29, 750–757.

Agrawal, R.K., 1987. A new equation for modeling nonisothermal kinetics. J. Therm. Anal. 32, 149–156.

Baqar, M., Agag, T., Ishida, H., Qutubuddin, S., 2011. Poly(benzoxazine-courethane)s: a new concept for phenolic/urethane copolymers via one pot method. Polymer 52, 307–317.

Chandramohan, A., Devaraju, S., Vengatesan, M.R., Alagar, M., 2012. Octakis(dimethylsiloxypropylglycidylether)silsesquioxane (OG-POSS) reinforced 1,1-bis(3-methyl-4-hydroxymethyl) cyclohexane based polybenzoxazine nanocomposites. J. Polym. Res. 19, 9903.

Chou, C.H., Hsu, S.L., Dinakaran, K., Chiu, M.Y., Wei, K.H., 2005a. Synthesis and characterization of luminescent polyfluorenes incorporating side-chain-tethered polyhedral oligomeric silsesquioxane units. Macromolecules 38, 745–751.

Chou, C.H., Hsu, S.L., Yeh, S.W., Wang, H.S., Wei, K.H., 2005b. Enhanced luminance and thermal properties of poly(phenylenevinylene) copolymer presenting side-chain-tethered silsesquioxane units. Macromolecules 38, 9117–9123.

Chozhan, C.K., Alagar, M., Gnanasundaram, P., 2009. Synthesis and characterization of 1,1-bis(3-methyl-4-hydroxy phenyl)cyclohexane polybenzoxazine–organoclay hybrid nanocomposites. Acta Mater. 57, 782–794.

Cui, H.W., Kuo, S.W., 2012. Using a polyhedral oligomeric silsesquioxane surfactant and click chemistry to exfoliate montmorillonite. RSC Adv. 2, 12148–12152.

Cui, H.W., Kuo, S.W., 2013. Nanocomposites of polybenzoxazine and exfoliated montmorillonite using a polyhedral oligomeric silsesquioxane surfactant and click chemistry. J. Polym. Res. 20, 114.

Fu, H.K., Huang, C.F., Kuo, S.W., Lin, H.C., Yei, D.R., Chang, F.C., 2008. Effect of an organically modified nanoclay on low-surface-energy materials of polybenzoxazine. Macromol. Rapid Commun. 29, 1216–1220.

Garea, S.A., Iovu, H., Nicolescu, A., Deleanu, C., 2009. A new strategy for polybenzoxazine–montmorillonite nanocomposites synthesis. Polym. Test. 28, 338–347.

Holly, F.W., Cope, A.C., 1944. Condensation products of aldehydes and ketones with o-aminobenzyl alcohol and o-hydroxybenzylamine. J. Am. Chem. Soc. 66, 1875–1879.

Hu, Rong-zu, Shi, Qi-zhen, 2001. Thermal Analysis Kinetics. Science Press, Beijing.

Hu, W.H., Huang, K.W., Kuo, S.W., 2012. Heteronucleobase-functionalized benzoxazine: synthesis, thermal properties, and self-assembled structure formed through multiple hydrogen bonding interactions. Polym. Chem. 3, 1546–1554.

Huang, K.W., Kuo, S.W., 2010. High performance polybenzoxazine nanocomposites containing multifunctional polyhedral oligomeric silsesquioxane (POSS) with allyl groups. Macromol. Chem. Phys. 211, 2301–2311.

Huang, J.M., Kuo, S.W., Lee, Y.J., Chang, F.C., 2007. Synthesis and characterization of a vinyl-terminated benzoxazine monomer and its blends with poly(ethylene oxide). J. Polym. Sci. B 45, 644–653.

Ishida, H., 2011. In: Ishida, H., Agag, T. (Eds.), Handbook of Benzoxazine Resins. Elsevier, Amsterdam, pp. 1–81 (Ch. 1).

Ishida, H., Allen, D.J., 1996. Physical and mechanical characterization of near-zero shrinkage polybenzoxazines. J. Polym. Sci. B 34, 1019–1030.

Ishida, H., Low, H.Y., 1997. A study on the volumetric expansion of benzoxazine-based phenolic resin. Macromolecules 30, 1099–1106.

Jin, L., Agag, T., Ishida, H., 2010. Bis(benzoxazine-maleimide)s as a novel class of high performance resin: synthesis and properties. Eur. Polym. J. 46, 354–363.

Kanchanasopa, M., Yanumet, N., Hemvichian, K., Ishida, H., 2001. The effect of polymerization conditions on the density and T_g of bisphenol-A and hexafluoroisopropylidene-containing polybenzoxanines. Polym. Polym. Compos. 9, 367–375.

Kiskan, B., Ghosh, N.N., Yagci, Y., 2011. Polybenzoxazine-based composites as high-performance materials. Polym. Int. 60, 167–177.

Kuo, S.W., Liu, W.C., 2010. Synthesis and characterization of a cured epoxy resin with a benzoxazine monomer containing allyl groups. J. Appl. Polym. Sci. 117, 3121–3127.

Kuo, S.W., Wu, Y.C., Wang, C.F., Jeong, K.U., 2009. Low surface energy materials through mediated by hydrogen bonding interaction. J. Phys. Chem. C 113, 20666–20673.

Lin, Y.C., Kuo, S.W., 2011. Self-assembly and secondary structures of linear polypeptides tethered to polyhedral oligomeric silsesquioxane nanoparticle through click chemistry. J. Polym. Sci. A 49, 2127–2137.

Lin, Y.C., Kuo, S.W., 2012. Synthesis, self-assembly and secondary structures of linear polypeptides graft to polyhedral oligomeric silsesquioxane in the side chain through click chemistry. Polym. Chem. 3, 162–171.

Song, X.Y., Zhou, S.Z., Wang, Y.F., Kang, W.M., Cheng, B.W., 2012. Mechanical and electret properties of polypropylene unwoven fabrics reinforced with POSS for electret filter materials. J. Polym. Res. 19, 9812.

Su, Y.C., Kuo, S.W., Yei, D.R., Xu, H.Y., Chang, F.C., 2003. Thermal properties and hydrogen bonding in polymer blend of polybenzoxazine/poly(*N*-vinyl-2-pyrrolidone). Polymer 44, 2187–2191.

Sudo, A., Kudoh, R., Nakayama, H., Arima, K., Endo, T., 2008. Selective formation of poly(N, O-acetal) by polymerization of 1,3-benzoxazine and its main chain rearrangement. Macromolecules 41, 9030–9034.

Wang, C.F., Wang, Y.T., Tung, P.H., Kuo, S.W., Lin, C.H., Sheen, Y.C., Chang, F.C., 2006a. Fabrication of patterned superhydrophobic polybenzoxazine hybrid surfaces. Langmuir 22, 8289–8292.

Wang, C.F., Su, Y.C., Kuo, S.W., Huang, C.F., Sheen, Y.C., Chang, F.C., 2006b. Low-surface-free-energy materials based on polybenzoxazines. Angew. Chem. Int. Ed. 45, 2248–2251.

Wang, C.F., Chiou, S.F., Ko, F.H., Chen, J.K., Chou, C.T., Huang, C.F., Kuo, S.W., Chang, F.C., 2007. Polybenzoxazine as a mold-release agent for nanoimprint lithography. Langmuir 23, 5868–5871.

Wang, C.F., Wang, T.F., Liao, C.S., Kuo, S.W., Lin, H.C., 2011. Using pencil drawing to pattern robust superhydrophobic surfaces to control the mobility of water droplets. J. Phys. Chem. C 115, 16495–16500.

Wang, W.P., Ding, W.L., Yu, J., Fei, M., Tang, J.Y., 2012. Synthesis and characterization of a novel POSS/PS composite via ATRP of branched functionalized POSS. J. Polym. Res. 19, 9948.

Yang, P., Gu, Y., 2011. Synthesis and curing behavior of a benzoxazine based on phenolphthalein and its high performance polymer. J. Polym. Res. 18, 1725–1733.